DOI: 10.1002/ejic.200701073

Different Morphological Organic–Inorganic Hybrid Nanomaterials as Fluorescent Chemosensors and Adsorbents for Cu^{II} Ions

Soo Jin Lee,[a] Doo Ri Bae,[a] Won Seok Han,[a] Shim Sung Lee,[a] and Jong Hwa Jung*[a]

Keywords: Adsorbents / Chemosensors / Fluorescence / Nanomaterials / Silica / Nanotubes

Functionalized silica nanotubes (FSNT), functionalized mesoporous silica (FMS), and functionalized silica nanoparticles (FSNP-15) with an immobilized phenanthroline moiety as a fluorescent receptor were fabricated by a sol–gel reaction, and their binding abilities with metal ions were evaluated by fluorophotometry in water/acetonitrile (8:2, v/v) at pH 7. They selectively recognized Cu^{2+} ions among other metal cations such as Co^{2+}, Cd^{2+}, Hg^{2+}, Ni^{2+}, Fe^{3+}, Ag^{+}, Pb^{2+}, and Zn^{2+}, because the Cu^{2+} ion selectively binds to the nitrogen atoms of the phenanthroline moiety. Among the three silica nanomaterials with the immobilized receptor **1**, the sensitivity of FSNT for Cu^{2+} ions is better than those of FMS and FSNP-15, indicating that the adsorption capacity for metal ions is dependent on the shape and surface area of the supporting nanomaterials. FSNT (10 mg) adsorb 75% of the Cu^{2+} ions (2.0×10^{-4} mM) while FSNP-15 (10 mg) adsorb only 36%. The detection limit of FSNT for Cu^{2+} ions was ca. 3.0×10^{-8} M. FSNT and FMS can be easily renewed by treatment with a solution of HCl and tetrabutylammonium hydroxide.

Introduction

Fluorescent molecules for transition and heavy metal cation sensors such as Hg^{2+}, Cu^{2+}, Pb^{2+}, and Zn^{2+} ions have become increasingly important as tools for the quantitative and the qualitative monitoring of the target metal ions in many biological and environmental processes.[1–6] On the basis of the concepts of host–guest chemistry, cation sensing has recently risen to prominence in research devoted to the detection of designated species. An effective fluorescent chemosensor must convert the event of cation recognition by the ionophore into an easily monitored and highly sensitive light signal from the fluorophore.[7] As such a fluorogenic unit, phenanthroline dye has been used for conjugation with biomolecules for fluorescent probes[7–8] owing to its excellent fluorescence properties. Although the phenanthroline unit itself is generally fluorescent, the addition of guest ions to a solution of phenanthroline quenches the fluorescence emission of the phenanthroline by a reverse photoinduced electron transfer (PET) effect.

Recently, inorganic nanomaterials have found broad applications in biological and environmental fields such as biolabeling, imaging, drug delivery, separation processes, and optical sensing.[9–12] The size and shape of nanomaterials play important roles in determining their properties, as well as affecting their usefulness in various applications. However, inorganic nanomaterials have not been widely used directly for specific applications as they have no functional groups suitable for biological and environmental conjugations. Thus, introduction of functional groups onto the surface of inorganic nanomaterials is an important strategy for generating useful structures for environmental applications, such as optical sensing and removal of pollutants and toxic metal ions in wastewater. Previously, we and other groups reported optical sensing and separation of toxic metal ions by using organic–inorganic hybrid nanomaterials.[12,13] These chromogenic receptors immobilized on silica nanomaterials have selectively recognized and separated metal ions. Importantly, they can be renewed by suitable treatment for repeated detection and separation of metal ions.

Despite these advantages, there are few examples in the literature of optical sensing for metal ions using nanomaterials.[12] Furthermore, there have been no reports on the influence of the shapes or the surface areas of the nanomaterials used as supporting materials in detection and separation of metal ions. Therefore, using three different morphologies of silica nanomaterials as supporting structures, we have developed fluorescent immobilized phenanthroline silica nanostructures. Herein, we report their adsorption capacities along with their fluorescence responses upon the addition of various metal cations. Furthermore, we compare the effects of morphological differences in the silica nanomaterials on their capacity to adsorb metal ions.

[a] Department of Chemistry and Research Institute of Natural Sciences, Gyeongsang National University
Jinju, 660-701, Korea
Fax: +82-55-758-6027
E-mail: jonghwa@gnu.ac.kr
Supporting information for this article is available on the WWW under http://www.eurjic.org/ or from the author.

Results and Discussion

Fabrication of Functionalized Silica Nanomaterials

The phenanthroline derivative **1** was synthesized by condensation of aminopropylphenanthroline **3** with 3-(triethoxysilyl)propylisocyanate in pyridine as a solvent (Scheme 1). Silica nanotubes (SNT) and mesoporous silica were prepared by adaptation of synthetic methods published earlier.[12]

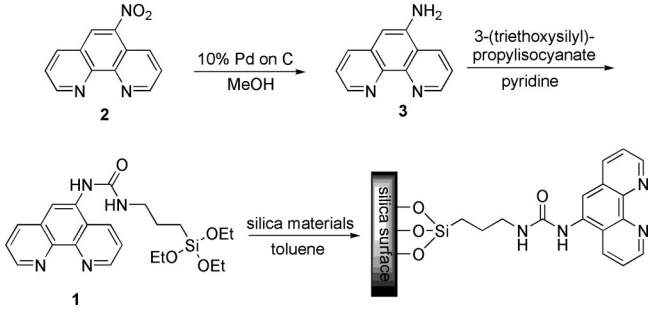

Scheme 1. Fabrication of organic–inorganic hybrid materials.

For comparison of their functional advantages to those of SNT and mesoporous silica, silica nanoparticles (SNP-15) with a diameter of 15 nm were purchased from Aldrich.

Phenanthroline derivative **1** was covalently attached onto the SNT, mesoporous silica, and SNP-15 by a sol–gel reaction in toluene (Scheme 1). The functionalized silica nanomaterials were well characterized by transmission electron microscopy (TEM), thermogravimetric analysis (TGA), FT-IR spectroscopy, and fluorophotometry.

The TEM pictures clearly show that SNT, mesoporous silica, and SNP-15 still retain their well-ordered nanostructures after attachment of phenanthroline derivative **1** (Figure 1). The modified silica products showed a well-defined nanotubular structure with a diameter of ca. 260 nm and a length of several micrometers (Figure 1a), a mesoporous structure with ca. 5.2 nm pore diameter (Figure 1b), and a spherical structure 15 nm in diameter (Figure 1c), respectively. Particularly the TEM images of FSNT and FMS displayed a hollow structure with uniform dimensions of size and diameter, indicating that fluorescent receptor **1** had covalently attached itself onto the surface of SNT and mesoporous silica by a sol–gel reaction.

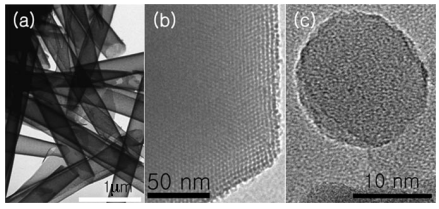

Figure 1. TEM images of (a) FSNT, (b) FMS, and (c) FSNP-15.

To gain insight into the changes in porosity induced by the introduction of phenanthroline derivative **1**, we measured the surface areas and the pore volumes before and after immobilization of **1** onto the surface of SNT, mesoporous silica, and SNP-15 with nitrogen adsorption–desorption isotherms.

BET (Brunauer–Emmett–Teller) surface areas were 800.2 m^2/g for SNT, 750.5 m^2/g for mesoporous silica, and 72.9 m^2/g for SNP-15 (Figure S1) before immobilization, whereas BET surface areas were 550.6 m^2/g for FSNT, 403.7 m^2/g for FMS, and 59.9 m^2/g for FSNP-15 after immobilization of receptor **1** (Figure 2), indicating that the surface areas of all modified supporting nanomaterials had decreased. In addition, from the results of TGA experiments (Figure S2), we noticed that **1** represents only 32 wt.-% and 23 wt.-% of FSNT and FMS, respectively, whereas FSNP-15 contain 16 wt.-% of **1**, obviously because silica nanoparticles have a much smaller surface area than either SNT or mesoporous silica.

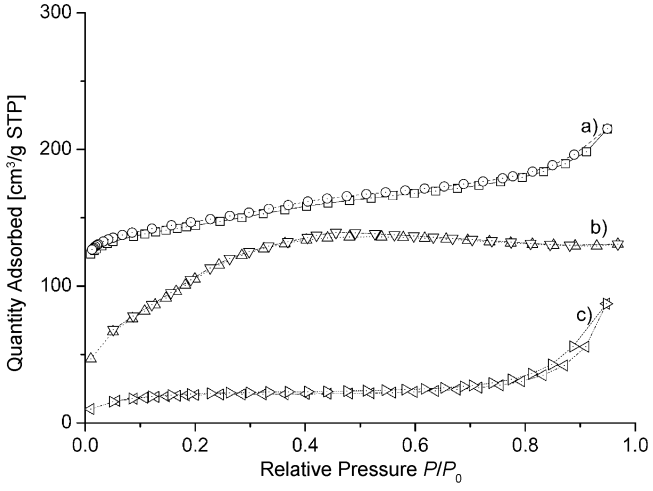

Figure 2. Nitrogen adsorption–desorption isotherms of (a) FSNT, (b) FMS, and (c) FSNP-15.

To obtain further structural proof for FSNT, we carried out IR spectroscopy for both SNT and FSNT. SNT have absorbances at 3430 and 1620 cm^{-1}, whereas FSNT exhibit the same absorbance bands as well as additional signals at 2976, 2933, 2884, 1643, 1570, 1471, 1446, and 1428 cm^{-1} (Figure S3). The new peaks originated from phenanthroline, giving solid evidence that **1** is attached onto the surface of the SNT. Also, we obtained similar IR spectra for FMS and FSNP-15 (see Exp. Sect.). Moreover, the strong fluorescence emission of FSNT, FMS, and FSNP-15 following excitation at 275 nm definitely arises from the introduction of **1** onto SNT, mesoporous silica, and SNP-15 (vide infra).

Binding Abilities of Functionalized Silica Nanomaterials with Metal Ions

We probed the binding abilities of FSNT and FMS for metal ions on the basis of changes in fluorescence upon the addition of Ag^+, Ni^{2+}, Fe^{3+}, Hg^{2+}, Co^{2+}, Cd^{2+}, Pb^{2+}, Zn^{2+}, and Cu^{2+} (all as nitrates) in water/acetonitrile (8:2, v/v) at pH 7 (Table 1 and Figure 3). In the absence of metal ions, excitation of solutions of equal concentrations of FSNT

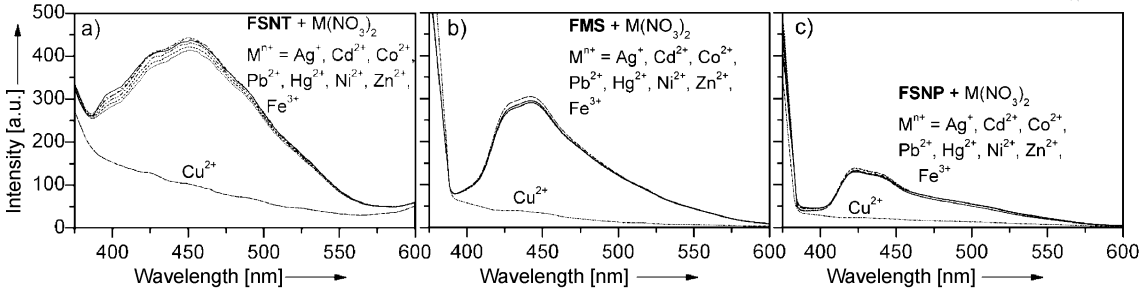

Figure 3. The emission spectra of (a) FSNT (0.30 mM), (b) FMS (0.30 mM), and (c) FSNP-15 (0.30 mM) upon the addition of metal nitrates (1.5 mM).

and FMS at 275 nm resulted in strong fluorescence emission bands (λ_{max} = 451 or 441 nm) arising from the covalently bound phenanthroline moiety (Figure 3). The fluorescence intensity of FSNT was slightly higher than that of FMS, because of the higher content of receptor **1** immobilized on FSNT.

Table 1. Fluorescence changes ($I - I_0$) for **1**, FSNT, FMS, and FSNP-15 upon addition of metal ions (1.5 mM).

	Fluorescence changes ($I - I_0$) [au]									
	λ_{em} [nm]	Ag^+	Cd^{2+}	Co^{2+}	Pb^{2+}	Hg^{2+}	Ni^{2+}	Zn^{2+}	Fe^{3+}	Cu^{2+}
1	411	–42	0	–6	–9	–21	–30	–21	–14	–306
FSNT	451	–42	0	0	–5	–12	–21	–21	–5	–340
FMS	441	–15	–2	–1	0	–8	–6	–5	–1	–270
FSNP-15	434	–7	–1	0	–1	–1	–3	–4	–1	–115

Interestingly, addition of Cu^{2+} to a suspension of FSNT or FMS in water/acetonitrile (8:2, v/v) markedly diminished the fluorescence intensity in FSNT or FMS (Figure 3a and Figure 3b), suggesting that Cu^{2+} formed a complex with the nitrogen atoms of the phenanthroline unit, and strongly quenched the emission intensity. In all cases, changes in fluorescence emission were found to be complete within 10 s. The fluorescence quenching can be explained as reverse photoinduced electron transfer when Cu^{2+}, bound to the nitrogen atoms of the phenanthroline unit, behaves as a PET donor.[12b,14] The fluorescence emission of the suspension of FSNT in water/acetonitrile (8:2, v/v) gradually decreases with increasing Cu^{2+} concentration (Figure S4), indicating that Cu^{2+} is quantitatively bound to the phenanthroline moiety attached to FSNT. In contrast, the fluorescence of FSNT and FMS did not change upon addition of Co^{2+}, Hg^{2+}, Ni^{2+}, Cd^{2+}, Pb^{2+}, Fe^{3+}, Ag^+, and Zn^{2+}. These results support the view that those metal ions did not bind to the phenanthroline moiety of FSNT and FMS. Gunnlaugsson et al. recently reported the highly selective colorimetric naked-eye detection of copper ions by using an azobenzene chemosensor, {carboxymethyl[2-methoxy-4-(4-nitro-phenylazo)-phenyl]amino}acetic acid dipotassium salt.[6g] In their study, the azobenzene chemosensor showed a high selectivity and sensitivity for Cu^{2+} with an iminodiacetate receptor, which was introduced to provide an extra chelating site especially for Cu^{2+}. In addition, they also indicate that both Zn^{2+} and Cd^{2+} modulate the adsorption spectra. However, these changes occur at much higher concentrations than that of Cu^{2+}. Therefore, it is probably possible that a significant fluorescence change for FSNT and FMS could occur upon addition of Ag^+, Ni^{2+}, and Zn^{2+} ions at much higher concentrations than that for Cu^{2+} (Table 1).

Similarly, the selectivity of the fluorescence response of FSNP-15 for metal ions was almost the same as that of FSNT or FMS (Figure 3). The fluorescence response was quenched by a factor of ca. 3 upon addition of Cu^{2+} (1.5 mM) for **1**, FSNT, FMS, and FSNP-15, over almost the same dynamic range. However, the intensity of Cu^{2+}-bound FSNP-15 was ca. 3.1-fold lower relative to that of Cu^{2+}-bound FSNT, because of the lower content of receptor **1** immobilized on FSNP-15. Also, SNP-15 are more agglomerated in comparison to SNT even though SNP-15 have nanosize diameter. Agglomeration of the nanoparticles would induce a lower content of receptor **1** on the surface of FSNP-15 because of the reduced specific surface area of FSNP-15. Thus, these findings indicate that SNT are much more useful as a supporting solid nanomaterial in comparison to a spherical nanomaterial.

We examined the recovery of the phenanthroline-modified silica nanomaterials after exposure to copper ions.[15] The FSNT–Cu^{2+} were treated with a 0.1 N solution of HCl and then neutralized with 0.1 N tetrabutylammonium hydroxide (TBA^+OH^-) (Figure 4). Interestingly, we found that the fluorescence of FSNT increases upon addition of the base. As shown in Figure 4B, the decrease in fluorescence upon exposure to copper ions was fully reversible, as the addition of strong base to the acidic solution reversed this

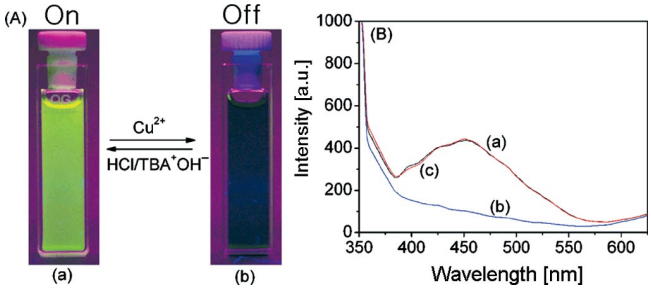

Figure 4. (A) Picture of FSNT (a) without and (b) with Cu^{2+} ions under irradiation from a UV-lamp. (B) Fluorescent spectra of FSNT (0.30 mM) (a) without and (b) with Cu^{2+} ions, and (c) after treatment with HCl/TBA^+OH^- in (b) solution.

effect. In addition, the fluorescence change was reproducible over several cycles of detection–separation. These results clearly indicate that the phenanthroline-modified silica nanomaterials are stable in operating conditions. With the observed fluorescence on–off–on behavior upon metal and then acid/base treatment, we are sure that FSNT can be recycled for environmental usage.

In control studies, changes in fluorescence upon the addition of metal ions for **1** and for SNT alone, without the covalently attached phenanthroline units, were measured. As shown in Figures S5 and S6, the fluorescence of **1** dramatically decreased with the addition of only Cu^{2+}, but did not change with the addition of any other metal ions. Also, no changes in fluorescence were observed upon the addition of any metal ions to unmodified SNT. Thus, it can be concluded that Cu^{2+} is selectively bound to nitrogen atoms of the phenanthroline unit on the surface of FSNT.

In efforts to understand the coordination behavior between receptor **1** attached to FSNT and Cu^{2+}, our repeated attempts to obtain the crystal structures of the related complexes were not successful. As an alternative, we measured FT-IR spectra of both Cu^{2+}-free FSNT and Cu^{2+}-bound FSNT to confirm the binding site of Cu^{2+}. The characteristic peak due to –N–C groups in **1** at 1385 cm^{-1} shifted to 1377 cm^{-1} when complexed with Cu^{2+} (Figure S7). The resulting shift to shorter wavenumbers is attributed to the coordination of the Cu^{2+} ion to the nitrogen atoms in the phenanthroline moiety. Furthermore, the molecular weight of the **1**–Cu^{2+} complex was measured by FAB mass spectroscopy (Figure S8). As shown in Figure S8, evidence for the 3:1 complex was indicated by the FAB mass spectrum of the $[\mathbf{1}]_3$–Cu^{2+} complex (*m*/*e* = 694). However, it is not clear that these results gave direct evidence for the 3:1 complex, because other binding sites, such as the amide moiety and the silica surface, seem to operate in this case. The binding ability of the amide moiety in this fashion was also observed in the azobenzene-coupled chromogenic receptors for the selective detection of Cu^{2+}.[6a] Evidence for coordination between Cu^{2+} and the phenanthroline receptor **1** attached to SNT was further confirmed by the EDX technique (Figure S9). The material contained silicon, carbon, nitrogen, and copper components, supporting the idea that Cu^{2+} ions are homogenously adsorbed by electrostatic interaction with **1**, which is covalently attached in FSNT.

We obtained the standard calibration data (FSNT fluorescence intensity vs. $[Cu^{2+}]$) for the concentration of the Cu^{2+} ion (Figure S10). The data did not exactly obey a linear relationship, probably because Cu^{2+} can principally form three different complexes, **1**:Cu^{2+} = 3:1, 2:1, and 1:1. The changes in the fluorescence of FSNT with changes in $[Cu^{2+}]$ were observed between $[Cu^{2+}]$ values of ca. 3.0×10^{-8} M and ca. 1.0×10^{-6} M with a detection limit of ca. 3.0×10^{-8} M.

Adsorption Capacities of Functionalized Silica Nanomaterials for Metal Ions

The adsorption capacities of FSNT, FMS, and FSNP-15 for heavy metals were also estimated by ion chromatography (Figure 5 and Figure 6a). We observed that FSNT (10 mg) and FMS (10 mg) adsorb 75% and 52% of the

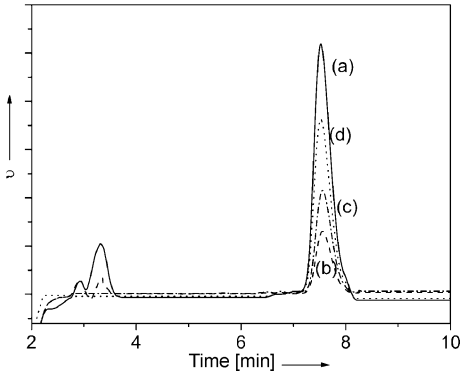

Figure 5. Ion chromatograms of Cu^{2+} (a) before and after extraction with (b) FSNT, (c) FMS, and (d) FSNP-15 in water/acetonitrile (8:2, v/v) at pH 7.

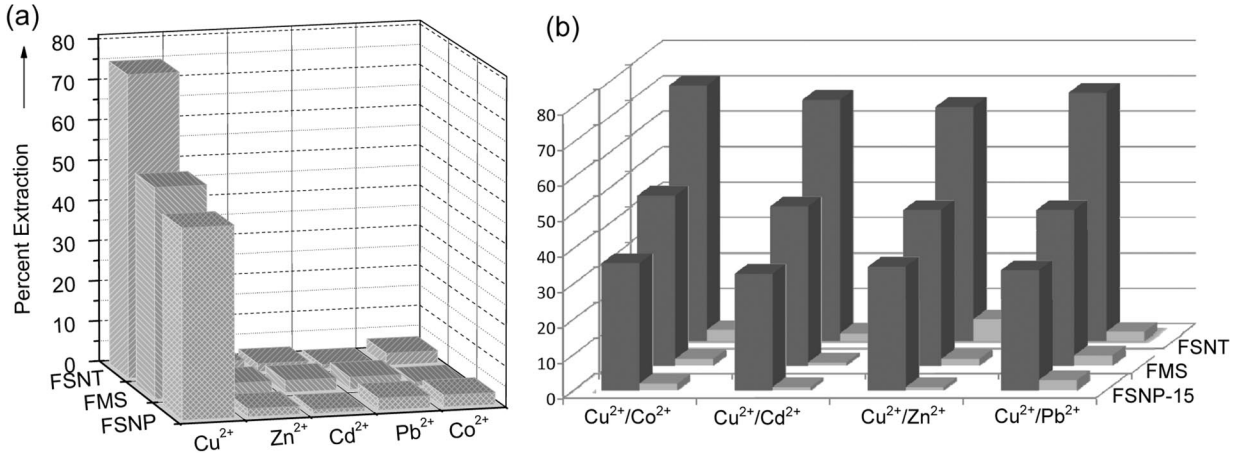

Figure 6. (a) Adsorption capacities of FSNT, FMS, and FSNP-15 for metal ions (all at a concentration of 2.0×10^{-4} M) in a single-ion system in water/acetonitrile (8:2, v/v) at pH 7. (b) Adsorption capacities of FSNT, FMS, and FSNP-15 for metal ions (all at a concentration of 2.0×10^{-4} M) in a binary-ion system in water/acetonitrile (8:2, v/v) at pH 7.

Cu^{2+} ions (2.0×10^{-4} mM) in a single-ion system, respectively, indicating that FSNT are better adsorbents than FMS for the separation of the Cu^{2+} ion. The higher adsorption capacity of FSNT for Cu^{2+} is due to the higher amount of receptor **1** on the FSNT surface. In addition, FSNT were well dispersed in the solvent. In contrast, in single-ion systems, less than 5% of other metal ions Zn^{2+}, Cd^{2+}, Co^{2+}, and Pb^{2+} (all with a concentration of 2.0×10^{-4} mM) were extracted into the solid phase. Furthermore, FSNP-15 (10 mg) showed much lower (36%) extractability for Cu^{2+} (2.0×10^{-4} mM) than did FSNT and FMS. Thus, FSNT are potentially useful as metal adsorbents for Cu^{2+} in solid–liquid extraction.

In addition, the adsorption capacities of FSNT, FMS, and FSNP-15 were measured through solid extraction by using solutions of binary metal systems: Cu^{2+}/Co^{2+}, Cu^{2+}/Cd^{2+}, Cu^{2+}/Zn^{2+}, and Cu^{2+}/Pb^{2+} (all at a concentration of 2.0×10^{-4} mM). 72–65%, and 45–40% of Cu^{2+} was adsorbed by FSNT (10 mg) and FMS (10 mg), respectively (Figure 6b). In contrast, in the binary systems, less than 1.3–6.0% of the competing metal ions, such as Co^{2+}, Cd^{2+}, Zn^{2+}, and Pb^{2+}, were extracted into the solid phase. The results suggest that FSNT are useful as adsorbents for the separation of Cu^{2+} in the presence of a range of heavy metal ions.

Conclusions

We have designed and fabricated FSNT and FMS, which incorporated a fluorescent phenanthroline receptor. FSNT and FMS recognized and separated Cu^{2+} with a high degree of selectivity from other metal ions. These organic–inorganic hybrid nanomaterials can be used for the separation and sensing of Cu^{2+} in environmental pollutants. Particularly, the adsorption capacity of FSNT for Cu^{2+} (75%) is better than those of FMS (52%) and FSNP-15 (36%), because of a larger surface area and good dispersion in solvents. Not unexpectedly, these findings indicate that the shape and surface area of supporting materials influence the adsorption capacity of metal ions. The effective use of FSNT and FMS sensors as remote sensing operators on a real-time basis would significantly open up general yet simple approaches for the identification of various biological and chemical toxic ions without using sophisticated instruments. Furthermore, these findings may lead to the development of a new type of tailor-made selective ion-sensing system built by finely controlling the properties of both the molecular receptor and the solid support.

Experimental Section

General: All reagents were purchased from Aldrich or Tokyo Kasei Chemicals and used without further purification.

Characterization: ^1H and ^{13}C NMR spectra were measured with a Bruker 300 apparatus. IR spectra were obtained for KBr pellets, in the range 400–4000 cm^{-1}, with a Shimadzu FT-IR 8400S instrument, and the MS spectrum was obtained with a JEOL JMS-700 mass spectrometer. Transmission electron microscopy (TEM) images were taken with a JEOL JEM-2100 F instrument operated at 50 keV. Images were recorded on an imaging plate (Fuji Photo Film Co. Ltd. FDL5000 system) with 20 eV energy windows at 3000–250000× magnification and were digitally enlarged. EDX analysis was performed with a JEOL ultra-thin-window (UTW) type EDX detector capable of detecting boron and an OXFORD EDS system for signal processing in a 180-s lifetime. Nitrogen adsorption isotherms were measured at 78 K with a Micromeritics ASAP 2020 analyzer. Thermal gravimetric analysis (TGA) was performed with a TA SDT Q600 instrument by using a heating rate of 10 °C/min with a Pt pan in air. The scanning range was from 25 to 900 °C.

Silica Nanotubes (SNT), Mesoporous Silica, and Silica Nanoparticles (SNP-15): The silica nanotubes and mesoporous silica were prepared by adaptation of synthetic methods published earlier.[12,16,17] The silica nanoparticles with 15 nm diameter were purchased from Aldrich.

Preparation of FSNT, FMS, and FSNP-15: Phenanthroline derivative **1** (50 mg, 0.05 mmol) was dissolved in anhydrous toluene (5 mL) to which silica nanomaterial (100 mg) was added, and it was stirred under reflux in N_2 for 24 h. The collected solid was washed several times with dichloromethane and acetone to rinse away any excess **1**. FSNT, FMS, or FSNP-15 were obtained as solids (100 mg). IR (KBr): $\tilde{\nu}$ = FSNT: 2976, 2933, 2884, 1643, 1570, 1471, 1446, 1428; FMS: 2970, 2933, 2883, 1640, 1570, 1475, 1446, 1429; FSNP-15: 2975, 2931, 2884, 1642, 1571, 1471, 1445, 1427 cm^{-1}.

Fluorescence Investigation: Fluorescence emission spectra were recorded with a Shimadzu RF-5301-PC instrument. Stock solutions (0.01 M) of the hydrated metal nitrate salts were prepared in H_2O/CH_3CN (8:2, v/v) at pH 7. Stock solutions of FSNT, FMS, or FSNP-15 were prepared in H_2O/CH_3CN (8:2, v/v). For all measurements, excitation was at 275 nm, with excitation and emission slit widths of 1.5 nm. The pH value was adjusted by using 3-morpholinopropane sulfonic acid, MOPS (0.2-M, pH 7).

Adsorption Capacities of FSNT, FMS, and FSNP-15 for Metal Ions: A H_2O/CH_3CN (8:2, v/v, pH 7) solution of metal ions (2.0×10^{-4} mmol) with FSNT (10 mg), FMS (10 mg), or FSNP-15 (10 mg) was stirred for 10 min at room temperature. After filtration, the concentration of metal ions remaining in the organic phase was analyzed by ion chromatography (DX–500, DIONEX).

Preparation of Compound 1: A solution of **3** (175 mg, 0.9 mmol) in pyridine (5 mL) at 80 °C was treated with 3-(triethoxylyl)propylisocyanate (115 mg, 1.17 mmol). The reaction mixture was stirred overnight at 80 °C, and then cooled to room temperature. After removal of solvent, the crude product was purified by flash column chromatography on aluminum oxide, by elution with ethyl acetate to provide the title compound (215 mg, 81%). ^1H NMR (300 MHz, $CDCl_3$, 25 °C): δ = 8.72 (d, 1 H), 8.57 (d, 1 H), 7.74 (d, 1 H), 7.39 (d, 1 H), 7.22 (d, 1 H), 6.75 (d, 1 H), 3.77 (m, 6 H), 3.13 (d, 1 H), 1.45 (m, 2 H), 1.18 (m, 9 H), 0.84 (m, 2 H) ppm. ^{13}C NMR (75 MHz, $CDCl_3$, 25 °C): δ = 146, 145, 141, 136, 132, 130, 128, 122, 120, 118, 115 ppm. MS (FAB) (%): m/z = 443 $[M + H]^+$. $C_{22}H_{30}N_4O_4Si$ (442.58): calcd. C 59.70, H 6.83, N 12.66; found C 60.21, H 6.51, N 12.11.

Compound 3: Compound **2** (200 mg, 0.89 mmol) was diluted in methanol (5 mL). After 5 min of N_2 purging, Pd on activated carbon (10 wt.-%, 40 mg) was added to compound **2** in solution. Under H_2 (3 atm), the reaction was allowed to proceed for 1 h. After filtration by Celite 545 and concentration, compound **3** was ob-

tained as a yellow solid (173 mg, quantitative yield). ^{1}H NMR (300 MHz, $CDCl_3$, 25 °C): δ = 8.75 (d, 1 H), 8.55 (d, 1 H), 7.73 (d, 1 H), 7.46 (d, 1 H), 7.26 (d, 1 H), 6.80 (d, 1 H), 5.20 (s, 2 H) ppm. ^{13}C NMR (75 MHz, $CDCl_3$, 25 °C): δ = 146, 145, 141, 136, 132, 130, 128, 122, 120, 118, 115 ppm. MS (FAB) (%): *m*/*z* = 196 [M + H]$^+$. $C_{12}H_9N_3$ (195.22): calcd. C 73.83, H 4.65, N 21.52; found C 73.61, H 4.51, N 21.22.

Supporting Information (see footnote on the first page of this article): N_2 adsorption–desorption isotherms of SNT, mesoporous silica, and SNP-15, TGA curves of FSNT, FMS, and FSNP-15, FT-IR spectra of SNT and FSNT, fluorescence spectra, in the presence of various amounts of metal ions, of FSNT, **1**, and SNT, FT-IR spectra of free and Cu^{2+}-bound FSNT, FAB-MS of **1** + Cu^{2+}, EDX mapping of FSNT + Cu^{2+}, and calibration curve for [Cu^{2+}].

Acknowledgments

This work was supported by a Korea Research Foundation Grant (KRF-2005-070-C00068) and a Korea Science and Engineering Foundation Grant (R01-2005-000-10229-0). In addition, this work was partially supported by the Korea Ministry of Environment as part of "The Eco-technopia 21 Project".

[1] a) J. Waluk, *Conformational Analysis of Molecules in Excited States*, Wiley-VCH, New York, **2000**; b) J. P. Desvergne, A. W. Czarnik, *Chemosensors of Ion and Molecule Recognition*, Kluwer, Dordrecht, **1997**; c) A. W. Czarnik, *Fluorescent Chemosensors for Ion and Molecule Recognition*, American Chemical Society, Washington, DC, **1993**.

[2] a) A. J. Bryan, A. P. de Silva, S. A. de Silva, R. A. D. D. Rupasinghe, K. R. A. S. Sandanayake, *Biosensors* **1989**, *4*, 169–179; b) C. C. Woodroofe, S. J. Lippard, *J. Am. Chem. Soc.* **2003**, *125*, 11458–11459.

[3] a) S. K. Kim, S. H. Lee, J. Y. Lee, R. A. Bartsch, J. S. Kim, *J. Am. Chem. Soc.* **2004**, *126*, 16499–16505; b) S. K. Kim, S. H. Kim, H. J. Kim, S. H. Lee, S. W. Lee, J. Ko, R. A. Bartsch, J. S. Kim, *Inorg. Chem.* **2005**, *44*, 7866–7875.

[4] a) S. J. Lee, J. H. Jung, J. Seo, I. Yoon, K.-M. Park, L. F. Lindoy, S. S. Lee, *Org. Lett.* **2006**, *8*, 1641–1643; b) M. K. Nazeeruddin, D. Di Censo, R. Humphry-Baker, M. Grätzel, *Adv. Funct. Mater.* **2006**, *16*, 189–194.

[5] a) R. Métivier, I. Leray, B. Lebeau, B. Valeur, *J. Mater. Chem.* **2005**, *15*, 2965–2973; b) E. Coronado, J. R. Galan-Mascaros, C. Marti-Gastaldo, E. Palomares, J. R. Durrant, R. Vilar, M. Grätzel, M. K. Nazeeruddin, *J. Am. Chem. Soc.* **2005**, *127*, 12351–12356.

[6] a) S. J. Lee, S. S. Lee, I. Y. Jeong, J. Y. Lee, J. H. Jung, *Tetrahedron Lett.* **2007**, *48*, 393–396; b) Y.-Q. Weng, F. Yue, Y.-R. Zhong, B.-H. Ye, *Inorg. Chem.* **2007**, *46*, 7749–7755; c) Z.-C. Wen, R. Yang, H. He, Y.-B. Jiang, *Chem. Commun.* **2006**, 106–108; d) S. H. Kim, J. S. Kim, S. M. Park, S.-K. Chang, *Org. Lett.* **2006**, *8*, 371–374; e) X. Qi, E.-J. Jun, L. Xu, S.-J. Kim, J. S. Hong, Y. J. Yoon, J. Yoon, *J. Org. Chem.* **2006**, *71*, 2881–2884; f) Z. Xu, X. Qian, J. N. Cui, *Org. Lett.* **2005**, *7*, 3029–3032; g) T. Gunnlaugsson, J. P. Leonard, N. S. Murray, *Org. Lett.* **2004**, *6*, 1557–1560; h) Y. Zheng, X. Cao, J. Orbulescu, V. Konka, F. M. Andreopoulos, S. M. Pham, R. M. Leblanc, *Anal. Chem.* **2003**, *75*, 1706–1712; i) R. Krämer, *Angew. Chem. Int. Ed.* **1998**, *37*, 772–773.

[7] a) H. Nohta, H. Satozono, K. Koiso, H. Yoshida, J. Ishida, M. Yamaguchi, *Anal. Chem.* **2000**, *72*, 4199–4204; b) A. Okamoto, T. Ichiba, I. Saito, *J. Am. Chem. Soc.* **2004**, *126*, 8364–8365.

[8] K. K.-W. Lo, C.-K. Chung, N. Zhu, *Chem. Eur. J.* **2003**, *9*, 475–483.

[9] K. K.-W. Lo, D. C.-M. Ng, W.-K. Hui, K.-K. Cheung, *J. Chem. Soc., Dalton Trans.* **2001**, 2634–2640.

[10] a) A. P. Wight, M. E. Davis, *Chem. Rev.* **2002**, *102*, 3589–3614; b) E. Topoglidis, C. J. Campbell, E. Palomares, J. R. Durrant, *Chem. Commun.* **2002**, 1518–1519; c) C.-Y. Lai, B. G. Trewyn, D. M. Jeftinija, K. Jeftinija, S. Xu, S. Jeftinija, V. S.-Y. Lin, *J. Am. Chem. Soc.* **2003**, *125*, 4451–4459; d) M. Numata, C. Li, A.-H. Bae, K. Kaneko, K. Sakurai, S. Shinkai, *Chem. Commun.* **2005**, 4655–4657.

[11] a) E. Palomares, R. Vilar, A. Green, J. R. Durrant, *Adv. Funct. Mater.* **2004**, *14*, 111–115; b) S. J. Son, S. B. Lee, *J. Am. Chem. Soc.* **2006**, *128*, 15974–15975; c) T. Balaji, S. A. El-Safty, H. Matsunaga, T. Hanaoka, F. Mizukami, *Angew. Chem. Int. Ed.* **2006**, *45*, 7202–7208.

[12] a) S. J. Lee, J.-E. Lee, J. Seo, I. Y. Jeong, S. S. Lee, J. H. Jung, *Adv. Funct. Mater.* **2007**, *17*, 3441–3446; b) S. J. Lee, S. S. Lee, M. S. Lah, J.-M. Hong, J. H. Jung, *Chem. Commun.* **2006**, 4539–4541; c) S. J. Lee, S. S. Lee, J. Y. Lee, J. H. Jung, *Chem. Mater.* **2006**, *18*, 4713–4715; d) T. H. Kim, J. H. Jung, J. K. Choi, Y. H. Choi, S. J. Lee, M. L. Seo, J. S. Kim, *Chem. Lett.* **2007**, *36*, 360–361; e) A. B. Descalzo, R. Martínez-Máñez, F. Sancenón, K. Hoffmann, K. Rurack, *Angew. Chem. Int. Ed.* **2006**, *45*, 5924–5948; f) F. Mancin, E. Rampazzo, P. Tecilla, U. Tonellato, *Chem. Eur. J.* **2006**, *12*, 1844–1854; g) R. Martínez-Máñez, F. Sancenón, *Chem. Rev.* **2003**, *103*, 4419–4476.

[13] a) A. B. Descalzo, K. Rurack, H. Weisshoff, R. Martínez-Máñez, M. D. Marcos, P. Amorós, K. Hoffmann, J. Soto, *J. Am. Chem. Soc.* **2005**, *127*, 184–200; b) E. Aznar, R. Casasús, B. García-Acosta, M. D. Marcos, R. Martínez-Máñez, F. Sancenón, J. Soto, P. Amorós, *Adv. Mater.* **2007**, *19*, 2228–2231.

[14] a) A. K. Patra, M. Nethaji, A. R. Chakravarty, *J. Inorg. Biochem.* **2007**, *101*, 233–244; b) X.-L. Wang, H.-Y. Lin, T.-L. Hu, J.-L. Tian, X.-H. Bu, *J. Mol. Struct.* **2006**, *798*, 34–39; c) Y.-Q. Wei, K.-C. Wu, B.-T. Zhuang, Z.-F. Zhou, *J. Coord. Chem.* **2006**, *59*, 713–719; d) M. D. Stephenson, M. J. Hardie, *Cryst. Growth Des.* **2006**, *6*, 423–432.

[15] R. C. Major, X.-Y. Zhu, *J. Am. Chem. Soc.* **2003**, *125*, 8454–8455.

[16] a) J. H. Jung, K. Yoshida, T. Shimizu, *Langmuir* **2002**, *18*, 8724–8727; b) J. H. Jung, Y. Ono, S. Shinkai, *Langmuir* **2000**, *16*, 1643–1649.

[17] a) D. Zhao, J. Feng, Q. Huo, N. Melosh, G. H. Fredrickson, B. F. Chmelka, G. D. Stucky, *Science* **1998**, *279*, 548–552; b) Y. Sakamoto, M. Kaneda, O. Terasaki, D. Y. Zhao, J. M. Kim, G. Stucky, R. Ryoo, *Nature* **2000**, *408*, 449–453.

Received: October 4, 2007
Published Online: February 18, 2008

